

# Review

Genotypic, Proteomic, and Phenotypic Approach to Decipher the Response to Caspofungin Drug and Calcineurin Inhibitors in Echinocandin-Resistant *Candida glabrata*.

Files

Details

Authors

Subjects

Declarations

Review

Saved 1 minute ago

## Files

Edit

### 4 FILES ADDED

Manuscript

Ceballos et al 2021 C. glabrata.docx

Supplementary File 1

Table S1. label\_free\_Total proteins.xlsx

Supplementary File 2

table S2. Description of the differentially abundant proteins after caspofungin treatment.xlsx

Supplementary File 3

### ARTICLE TYPE

Original Research

### TITLE

Genotypic, Proteomic, and Phenotypic Approach to Decipher the Response to Caspofungin Drug and Calcineurin Inhibitors in Echinocandin-Resistant *Candida glabrata*.

### ABSTRACT

Echinocandin resistance is a great concern, considering that these drugs are recommended as first-line therapy for invasive candidiasis. Its resistance is conferred by mutations in FKS genes. Nevertheless, pathways that regulate cellular stress responses could be crucial for enabling tolerance, evolution, and maintenance of drug resistance.

Here we identify resistant mechanisms by whole genome sequencing in echinocandin-resistant *C. glabrata*, followed by studies of quantitative proteomic response to caspofungin exposure and the analysis of the impact of calcineurin inhibition were conducted. After analyzing several genes related to caspofungin resistance, F659-del was found in the FKS2 gene of resistant strains. Regarding proteomics data, some up-regulated proteins are involved in cell wall biosynthesis, response to stress and pathogenesis, some of them being members of calmodulin-calcineurin pathway. Therefore, the impact of calmodulin and calcineurin inhibitors on susceptibility, stress tolerance, biofilm formation, and pathogenicity were explored. These inhibitors allow caspofungine susceptibility restoration, decrease of capacity to respond to stress conditions, reduction of biofilm formation and in vivo pathogenicity. In conclusion, our findings confirm that calmodulin-calcineurin-Crz1 could provide a relevant target in life-threatening fungal infectious diseases.

Give Feedback

Give Feedback

## Track your submissions

**Genotypic, Proteomic, and Phenotypic Approach to Decipher the Response to Caspofungin Drug and Calcineurin Inhibitors in Echinocandin-Resistant *Candida glabrata*.**

Amendment received 1 minute ago

Corresponding Author: Claudia M Parra Giraldo

Scientific Reports

e455638a-1c4b-4b73-a853-d69384173098 | v1.1

Don't forget, if you have manuscripts with other systems, such as eJournalPress or Editorial Manager, you will only be able to see those manuscripts there. Still have a question? [Contact us](#)

**Genotypic, Proteomic, and Phenotypic Approach to Decipher the  
Response to Caspofungin Drug and Calcineurin Inhibitors in  
Echinocandin-Resistant *Candida glabrata*.**

Andres Ceballos-Garzon <sup>1,2</sup>, Lucia Monteoliva<sup>3</sup>, Concha Gil<sup>3,4</sup>, Carlos Alvarez-Moreno<sup>5</sup>,  
Nelson E. Vega-Vela<sup>1</sup>, David M. Engelthaler<sup>6</sup>, Jolene Bowers<sup>6</sup>, Patrice Le Pape<sup>2§</sup>, Claudia  
M. Parra-Giraldo<sup>1§</sup>

<sup>1</sup>Unidad de Proteómica y Micosis Humanas, Grupo de Enfermedades Infecciosas  
Departamento de Microbiología, Facultad de Ciencias, Pontificia Universidad Javeriana,  
Bogotá D.C, Colombia.

<sup>2</sup>Department of Parasitology and Medical Mycology University of Nantes, Nantes  
Atlantique Universities, Faculty of Pharmacy, Nantes, France.

<sup>3</sup>Departamento de Microbiología y Parasitología, Facultad de Farmacia, Universidad  
Complutense de Madrid, Spain.

<sup>4</sup>Unidad de Proteómica, Universidad Complutense de Madrid, Spain.

<sup>5</sup>Department of Internal Medicine, Faculty of Medicine, Universidad Nacional de  
Colombia, Bogotá, Colombia; Clínica Universitaria Colombia, Clinica Colsanitas, Bogotá,  
Colombia.

<sup>6</sup>Translational Genomics Research Institute, Flagstaff, Arizona, USA.

§Corresponding authors at: Patrice.Le-Pape@univ-nantes.fr;  
Claudia.parra@javeriana.edu.co.

Word counts:

Abstract: 180 Body text: 2893

## Abstract

Echinocandin resistance is a great concern, considering that these drugs are recommended as first-line therapy for invasive candidiasis. Its resistance is conferred by mutations in *FKS* genes. Nevertheless, pathways that regulate cellular stress responses could be crucial for enabling tolerance, evolution, and maintenance of drug resistance. Here we identify resistant mechanisms by whole genome sequencing in echinocandin-resistant *C. glabrata*, followed by studies of quantitative proteomic response to caspofungin exposure and the analysis of the impact of calcineurin inhibition were conducted. After analyzing several genes related to caspofungin resistance, F659-del was found in the *FKS2* gene of resistant strains. Regarding proteomics data, some up-regulated proteins are involved in cell wall biosynthesis, response to stress and pathogenesis, some of them being members of calmodulin-calcineurin pathway. Therefore, the impact of calmodulin and calcineurin inhibitors on susceptibility, stress tolerance, biofilm formation, and pathogenicity were explored. These inhibitors allow caspofungine susceptibility restoration, decrease of capacity to respond to stress conditions, reduction of biofilm formation and *in vivo* pathogenicity. In conclusion, our findings confirm that calmodulin-calcineurin-Crz1 could provide a relevant target in life-threatening fungal infectious diseases.

**Keywords:** *Candida glabrata*, caspofungin resistance, calcineurin inhibitors, proteomic.

## Introduction

The echinocandins drugs are recommended as first-line therapy for invasive candidiasis because of their low toxicity and high efficacy, especially against azole-resistant *Candida* isolates<sup>1,2</sup>. Echinocandin resistance in *Candida spp*, being potentially associated with treatment failures, is conferred by mutations in "hot spot" regions of the target *FKS* genes that lead to amino acid substitutions in the 1,3- $\beta$ -D-glucan enzyme<sup>3,4</sup>. In *C. albicans*, substitutions in Ser641 and Ser645 are the most frequent *FKS* mutations and cause the more pronounced resistance phenotypes<sup>5</sup>. In *C. glabrata*, the principal reported substitutions were Ser629 in Fks1 Ser663 and Phe659 in Fks2<sup>3,6,7</sup>, while natural polymorphisms have been described in *C. parapsilosis* and *C. guilliermondii FKS1*<sup>8</sup>. The ultimate consequence of these mutations is a significant decrease in the echinocandin affinity for the enzyme target and high minimum inhibitory concentrations (MICs) values. It is of importance to highlight that in some resistant isolates, no *FKS* mutations were identified and isolates with the same *FKS* mutations exhibit different resistance profiles indicating that other resistance mechanisms and putative target genes could be implicated<sup>9</sup>. In addition to these described resistance mechanisms, there is also a new hypothesis in which regulators of cellular stress responses could be crucial for enabling the evolution and maintenance of drug resistance<sup>4,10,11</sup>. Indeed, some cellular stress responses are governed by signaling pathways, the most studied being the cAMP, the calmodulin-calcineurin (CaM/CaL), the TOR (target of rapamycin), and the mitogen-activated protein kinase (MAPK) signaling pathways<sup>11-14</sup>. The CaM/Cal pathway formed by a complex of the proteins Cnb1, Cna1, Hsp90 and the transcription factor Crz1 in yeast is involved in calcium homeostasis, sphingolipid and cell wall biosynthesis, protein trafficking, ubiquitin

82 signaling, autophagy, adaptation to environmental changes and even more importantly, in  
83 the response to antifungal drug pressure (11,14-19). Crz1 is found downstream in the  
84 CaM/Cal pathway and is one of the main antifungal targets since Crz1 is not present in  
85 human cells. Once the transcription factor is activated by dephosphorylation mediated by  
86 the CaM/Cal-Hsp90 complex, it moves to the cell nucleus. Crz1 contains a C2H2 zinc  
87 finger motif that binds to a specific calcineurin dependent response element (CDRE) in the  
88 gene promoters, thus initiating the activation of ~87 genes, among which is the *FKS2* gene,  
89 involved in the caspofungin resistance <sup>9,17</sup>.

90 The spread of antifungal resistance and the limited number of available antifungal drugs  
91 amplifies the need to identify new fungal targets for development of novel therapeutic  
92 alternatives. In this context, bearing in mind the biological importance and the multiple  
93 processes in which calcineurin is implicated, this protein has been proposed as a potential  
94 target for the design of new antifungals <sup>18</sup>.

95 Calcineurin inhibitors such as Tacrolimus (Fk506) and cyclosporine A (CsA), which bind  
96 to the immunophilins FKBP12 and cyclophilin A, respectively, are well recognized as  
97 immunosuppressive drugs with potential antifungal properties<sup>19,20</sup>.

98 In attempt to identify protein targets, proteomic approaches should be employed. This  
99 approach has been previously applied in *C. albicans* to study many aspects, including  
100 adaptive responses to osmotic stress, macrophage interaction, and antifungal exposure.  
101 These studies evidenced that pathways such as the MAPK signaling pathway played a  
102 significant role in all biological responses <sup>21-26</sup>. More recently, global proteomic analyses  
103 defined Hsp90 as a central hub of protein interaction networks, which include nuclear  
104 transport, metabolic enzyme and signaling. Furthermore, these studies revealed that a large

group of co-chaperones work together for stress regulation and contribution to drug tolerance<sup>27</sup>.

To our knowledge, few proteomic studies have been done in *C. glabrata*. Among them, studies explored the implication of hyperadhesive proteins in host-pathogen interaction and biofilm formation, mechanisms of drug resistance mainly in biofilms and response to antifungal drugs such as clotrimazole and 5-flucytosine<sup>28–31</sup>. However, similar approaches to study antifungal response to caspofungin have not been previously described.

Based on this, the first objective of the present study was to identify resistant mechanisms by whole genome sequencing in clinical echinocandin-resistant *C. glabrata* isolates. We then describe the proteomic response to caspofungin exposure and determine the impact of calcineurin inhibition by FK506 and CsA inhibitors on susceptibility, stress tolerance, biofilm formation, and assess pathogenicity in the *Galleria mellonella* model.

## **Results**

### **Whole genome sequencing reveals *FKS2* nucleotide deletion**

Twenty-five genes associated with antifungal drug resistance were screened for mutations (see Materials and Methods – Molecular Evaluation for the complete gene list) (**Table 1**). Although some mutations were identified in our resistant isolates (CAGL1256 and CAGL1875), only the *FKS2* gene exhibited a 3-nucleotide deletion (1974-CTT-1976), which has been previously reported to be associated with echinocandin-resistant phenotypes. All other observed mutations were found in both resistant and susceptible isolates. The 3-nucleotide deletion detected (**Figure 1A**), which preserves the same open reading frame, explained the single amino acid deletion at Fks2 (F659-del; see **Figure 1B**)

observed in the two resistant isolates. This amino acid deletion which confers resistance to the echinocandins, resides within the Fks2 hot spot 1 (**Figure 1C**).

**Proteomic analysis of resistant *C. glabrata* cells treated with caspofungin reveals an increase of proteins related to stress adaptation and wall organization**

A total of 1796 distinct proteins were identified (**Table S1**). While 1509 of them were encoded by uncharacterized ORFs, 287 were encoded by characterized genes. Among these proteins, 53 were identified as less abundant (i.e., downregulated) and 220 proteins were identified as more abundant (i.e., upregulated) after caspofungine exposure (change in abundance ratio: caspofungin/control).

However, only 21 proteins, including 5 upregulated and 16 downregulated, were significantly different if significance (>1.5-fold change and p-value <0.05). Using gene ontology enrichment tools, several GO terms were found to be enriched from these 21 proteins. In the molecular functions, 14 terms were enriched. Among them, MAP kinase activity, drug binding, calcium-serine/threonine, ATPase activity, and ATP-binding were over-represented. Regarding biological process categories, 18 terms were enriched, including signal transduction, pathogenesis, response to stress/drug and wall biogenesis were over-represented (**Figure 2A**). Downregulated proteins, following caspofungin exposure, were mainly of enzymatic group: CAGL0I03300g (homologue to *Candida albicans* Bud16, here named as (Ca.Bud16), CAGL0K07744g (Ca.Ysa1), CAGL0K05813g (Ca.Ttr1), CAGL0J06952g (Ca.Idi1), CAGL0H09218g (Cg.Sdt1). The protein with the most negative differential ratio was CAGL0M08514g (Cg.Pir5), a protein associated with  $\beta$ -1,3-glucan strengthening. The more abundant proteins after caspofungin exposure were involved in DNA binding i.e., CAGL0M06831g (Cg.Crz1) CAGL0J11440g (Ca.Srp1), CAGL0L10021g (Ca.Dbp5), CAGL0C01683g (Ca.Isw1). Of interest are the proteins

involved in antifungal response CAGL0M06831g (Cg.Crz1) (CaM/Cal pathway), CAGL0J00539g (Cg.Slt2) (PKC pathway), CAGL0J11440g (Ca.Srp1). The corresponding protein abundance is presented in (**Figure 2B**), and description of these proteins is provided in (**Table S2**). Additionally, the genes from the 5 most abundant proteins following caspofungin exposure were evaluated for mutations, however, none were observed.

Concerning the 220 more abundant proteins after caspofungin treatment (only change in abundance ratio) (**Table S3**), gene ontology enrichment tools, revealed several enriched GO terms. Eleven molecular function terms were enriched, among them, ATP-binding, drug binding, kinase activator activity, and calmodulin binding. Regarding the biological process categories, 11 terms were enriched, among them, response to stress, growth, and cell wall organization/biogenesis. By using word enrichment, words related to “resistance”, “integrity”, “calcineurin”, “stress” and “kinase” have emerged. Using the STRING tool, the diagram based on the *C. glabrata* proteomic findings after exposure to caspofungin identified relevant members of CaM/Cal (Cna1, Cnb1, Crz1) and PKC (Rho1, Pkc1, Slt2) pathways (**Figure 3**).

Considering the important role of the CaM/Cal pathway in antifungal response, and the significant change of Crz1 (to date there are no Crz1 inhibitors) after caspofungin exposure, we focused this study targeting up-stream CaM/Cal proteins using commercial inhibitors.

#### **Calcineurin inhibition restores susceptibility of caspofungin-resistant *C. glabrata***

Pharmacological inhibition of calcineurin by tacrolimus (Fk506) and cyclosporine (CsA) (15 µg/mL) did not show any statistically significant decrease of susceptible (0916 and ATCC2001) or resistant (CAGL1256 and CAGL1875) *C. glabrata* growth. By contrast, in



presence of caspofungin, the inhibitors Fk506 and CsA allowed susceptibility restoration of resistant clinical isolates with a significance reduction of the  $>16 \mu\text{g/mL}$  MIC values to 0.25 and 0.5  $\mu\text{g/mL}$  respectively (**Figure 4**).

#### **Response to oxidative stress is independent of caspofungin-resistance phenotype and not correlated with calcineurin signaling**

In order to understand the oxidative stress response in resistant *C. glabrata*, growth was assessed in presence of menadione, a cytotoxic quinone that generates superoxide. The four isolates grew in up to 0.2 mM menadione and addition of Fk506 and CsA did not show any significant modification. The significant growth reduction of the resistant isolate CAGL1875 suggested higher susceptibility to caspofungin in presence of 0.2 mM menadione. Since combinations of caspofungin and calcineurin inhibitors lead to complete growth inhibition out of any stress, the impact of 0.2 mM menadione addition could not be interpreted. In presence of 0.4 mM menadione, PUJ/HUSI 0916 and CAGL1256 strains maintained a similar growth rate, independent of the caspofungin resistance phenotype (**Figure 5A**).

#### **Calcineurin inhibitors compromise growth of caspofungin-resistant *C. glabrata* in heat-shock conditions**

The heat stress spot test at 37°C confirmed previous results concerning the effect of calcineurin inhibitors on caspofungin-resistant isolates (**Figure 4**). Heat shock at 40 °C did not have impact on isolate growth for all but ATCC 2021. Interestingly, at this temperature, the growth of caspofungin-resistant isolates was noticeably compromised by calcineurin inhibitors (**Figure 5B**).

## **Calcineurin inhibitors significantly reduces biofilm-forming capacity**

The four isolates had the capacity to form biofilm in polystyrene microplate wells, as on polyurethane catheter pieces, but biofilm formation was lower in the more clinically relevant catheter model. Caspofungin treatment reduced biofilm formation in susceptible isolates especially in catheter piece model whereas no significant activity was detected for resistant isolates (**Figure 6 A-B**). By contrast, addition of calcineurin inhibitors to caspofungin significantly reduced the capacity of biofilm formation of resistant isolates, regardless of the model used ( $p < 0.05$ ).

## **Calcineurin inhibition reduces *C. glabrata* pathogenicity in the invertebrate *Galleria mellonella*.**

*C. glabrata* isolates typically lead to complete mortality of *G. mellonella*, 4-6 days post-infection. Treatment with caspofungin (1  $\mu$ g/Larvae) increased the larva survival when infected with susceptible isolates but did not exhibit, as expected, any statistical modification for caspofungin-resistant isolates. However, addition of calcineurin inhibitors to caspofungin proved to be effective in prolonging survival ( $P < 0.05$ ). No larval mortality was observed in control larvae injected with an equivalent volume of PBS (**Figure 7**).

## **Discussion**

*C. glabrata* is one of the most prominent *Candida* species detected in bloodstream isolates worldwide, typically exhibiting intrinsic resistance to azoles<sup>32-35</sup>. Moreover, echinocandin resistance in *C. glabrata* has increased, causing a serious clinical challenge<sup>36</sup>. Different mechanisms of resistance to echinocandins have been described, mainly associated with *FKS* genes alterations<sup>6,9</sup>. In this work, we employ whole genome sequencing to provide a

view of mutations involved in clinical caspofungin-resistant isolates targeting genes previously associated with echinocandin resistance<sup>9,37,38</sup>. To date, only a single *FKS2* gene deletion associated with caspofungin resistance was found; however, a larger comprehensive comparative analysis is ongoing.

Herein, we describe the first proteome description of resistant *C. glabrata* after caspofungin exposure, allowing us to identify 21 upregulated proteins. Taking into account that inhibition of  $\beta$ -1,3-glucan biosynthesis is the principal mode of action of caspofungin, which results in osmotic disruption of the fungal cell<sup>39</sup>, enrichment of molecular function and biological processes pathways were associated, as expected, with antifungal response, cell wall biogenesis, PKC and CaM/Cal pathways modulation. These results, similar to those previously reported in *C. albicans*<sup>13,40</sup>, confirm the association of these processes in the tolerance of *C. glabrata* to echinocandin exposure. Furthermore, we observed that caspofungin exposure resulted in increased GO annotations related to stress adaptation such as chemical and cation homeostasis, wall organization or biogenesis and response to heat. This feature has been described by Hoehamer et al.,<sup>21</sup> as the important changes in the *C. albicans* proteome in response to ketoconazole, amphotericin B, and caspofungin treatments although in that study only antifungal-susceptible strains were included.

*C. glabrata* exposure to caspofungin resulted in an increased abundance of MAP kinase Slt2 and Crz1 proteins which, being part of PKC and CaM/Cal pathways, respectively, have been implicated in cell wall biogenesis and integrity. This compensation phenomenon, also observed in *Saccharomyces cerevisiae* and *C. albicans* (Mkc1), constitutes a mechanism of tolerance to caspofungin<sup>13,14,41,42</sup>. Mutants lacking *SLT2/MKC1* and *CRZ1* are both sensitive to echinocandins in *in vitro* assays<sup>14,43</sup>. Nevertheless, Slt2 mutants have

been described as hypervirulent<sup>44</sup>. Other 3 proteins (CAGL0C01683g, CAGL0L10021g, CAGL0J11440g) were found with higher abundance after exposure to caspofungin, however, these proteins have not been characterized in *C. glabrata* to date. The protein CAGL0C01683g (Isw1) in *C. albicans* and *S. cerevisiae* has been described as a chromatin remodeling factor involved in the repression of the initiation of transcription. Isw1 also works in parallel with the NuA4 and Swr1 complexes in the repression of stress-induced genes<sup>45</sup>. The protein CAGL0L10021g (C.a, S.c Dpb5) is an ATP-dependent cytoplasmic RNA helicase involved in translation termination along with Sup45p (eRF1); it also has a role in the cellular response to heat stress<sup>46</sup>. Finally, the protein CAGL0J11440g (C.a, Sc Srp1) (importin- $\alpha$ ) has nuclear import signal receptor activity and is involved in the degradation of proteins. Loss of Srp1 is lethal, although several temperature-sensitive mutants have been described<sup>47,48</sup>. Conversely, Pir5 protein was decreased in abundance in response to caspofungin exposure. Pir proteins are a structural constituent of cell wall and are associated with cell wall organization due to linkage to multiple  $\beta$ -1,3-glucan chains. The changes in cell wall composition of the Pir proteins are a consequence of the cell wall integrity pathway activation<sup>49-51</sup>. This decrease of Pir5 abundance appears to be part of a general compensatory mechanism in response to cell wall weakening caused by caspofungin; consequently, the cell increases chitin and/or mannan production, a phenomenon reported in *S. cerevisiae* and *Candida spp*<sup>49,52</sup>. In a recently published study, all *Candida* species tested, except *C. glabrata* and *C. parapsilosis*, demonstrated a compensatory increase in cell wall chitin content in response to caspofungin treatment, therefore in *C. glabrata* the increase in the mannan content appears to be a compensatory mechanism<sup>53</sup>.

Given the importance of CaM/Cal-Crz1 pathway in several biological processes, the impact of Fk506 and CsA calcineurin inhibitors was studied in temperature and oxidative stress conditions. Similar to previous studies, we confirm that CaM/Cal pathway is involved in thermotolerance, mainly at higher temperatures<sup>54</sup>. By contrast, according to our results, the inhibition of calcineurin does not appear to affect the growth of *C. glabrata* in oxidative stress. It is important to emphasize that the antioxidant capacity of *C. glabrata*, mainly associated with the catalase Cta1, is higher than that of *S. cerevisiae* and *C. albicans*. This catalase Cta1 is controlled by the transcription factors Yap1, Skn7, Msn2, and Msn4 and modulated by pathways other than the CaM /Cal pathway<sup>55</sup>.

Biofilm formation is another important factor in the understanding of cellular disruption. Biofilms are thought to provide ecologic advantages such as protection from the environment, nutrient availability, metabolic cooperation, and acquisition of new traits. In general, *C. glabrata* biofilms possessed a higher density of cells comparatively to *C. tropicalis* and *C. parapsilosis* (hyphal and blastoconidia mix) biofilms. This may be implicated in the typical high degree of resistance of *C. glabrata* biofilms to azole antifungals and amphotericin B<sup>56</sup>. Biofilm eradication as a therapeutic approach is generally effective using echinocandins, as long as the isolate is drug susceptible<sup>57</sup>. In our study, planktonic caspofungin-resistant isolates maintain this characteristic in biofilm community state, even in the presence of high doses of caspofungin. Nevertheless, this situation can be reversed by addition of CaM/Cal inhibitors, as we demonstrated in the clinical-relevant model using polyurethane catheter pieces.

In a repurposing strategy as alternative to conventional antifungal therapy against caspofungin-resistant *C. glabrata*, our results establish an important role for CaM/Cal

inhibitors. These highly encouraging results could be supported by the well-recognized regulation of multiple biological processes governed by the CaM/Cal-Crz1, including over-expression of the *FKS2* gene which is involved in the resistance to the echinocandins. Effect of Fk506 and CsA on heat-shock tolerance or susceptibility restoration of biofilm to caspofungin could contribute to their *in vivo* activity. Indeed, in an invertebrate *Galleria* model of disseminated caspofungin-resistant *C. glabrata* infection, addition of CaM/Cal inhibitors to caspofungine enhances its efficacy, allowing a significant increase in larval survival. This is in concordance with previous data showing the role of CaM/Cal pathway in virulence of fungal species<sup>54,58</sup>. Despite these promising findings, non-immunosuppressive analogs of both FK506 and CsA with no cross-activity with calcineurin in human cells must be developed<sup>19,59,60</sup>. With regards to the CaM/Cal pathway, the challenge also will lie in focusing on the transcription factor Crz1, as recently explored for *Rhizoctonia solani*<sup>61</sup>. Transcription factors are now attractive as antifungal drug targets since they are evolutionarily divergent between fungi and humans and therefore can be exploited as selective targets<sup>62</sup>.

In conclusion, this is the first work on caspofungin-resistant *C. glabrata* clinical isolates that includes phenotypic, proteomic, and genomic analysis of impact of CaM/Cal pathway inhibition. Our study provides proteomic evidence that select proteins in this pathway, such as Crz1, are more abundant after caspofungin exposure. In addition, inhibition of this pathway in the clinical isolates with an *FKS2* gene mutation changed their planktonic and biofilm susceptibility, thermotolerance, and finally pathogenicity. Furthermore, addition of CaM/Cal inhibitors to caspofungin restored the susceptibility of resistant isolates in an *in vivo* *Galleria* model. Synthesis of more specific antifungal compounds targeting this stress

response could be a successful therapeutic strategy for fighting life-threatening fungal diseases and increase of echinocandin resistance.

## **Materials and Methods**

### **Microorganisms**

One susceptible and two caspofungin-resistant *C. glabrata* isolates were studied. The first one, *C. glabrata* PUJ/HUSI 0916 was recovered from a blood culture of a hematopoietic stem cell transplant recipient admitted to the Hospital Universitario San Ignacio Bogota, Colombia. The caspofungin-resistant isolates CACG1875 and CACG1256 were obtained from blood and urine cultures of hospitalized patients in intensive care unit of Centre Hospitalier Universitaire de Nantes, France and identified by ITS sequencing in a previous study by our research team <sup>11</sup>. Isolates were categorized as susceptible or resistant to caspofungin according to the interpretative breakpoints of CLSI M60 2017 criteria (> 0.5 µg/mL resistant strain). In addition, the reference *C. glabrata* ATCC2001, *C. parapsilosis* ATCC 22019 and *C. krusei* ATCC 6258 were used in specific experiments, as described in results. In this investigation, no ethical approval was required. All patients are anonymized and only the code of strains was transferred, therefore, no informed consent was required. Our study confirmed that all methods were performed in accordance with the relevant guidelines and regulations.

### **Whole genome sequencing and identification of molecular resistance mechanism**

The whole genome of the susceptible (PUJ/HUSI 0916) and resistant (CACG1875 and CACG1256) *C. glabrata* isolates were sequenced using Illumina paired-end sequencing platform with a read length of 300bp and an average read depth coverage of 300X. The

obtained raw read sequences were cleaned using *fastp*<sup>63</sup> and assembled with SPAdes v3.12.0<sup>64</sup>. Gene prediction was carried out with Prodigal V2.6.3<sup>65</sup> and the coding sequences (CDS) obtained were annotated using *blastn*<sup>66</sup>, against the genome of *C. glabrata* ATCC2001 reference strain.

In this study, we decided to focus on the following twenty-five genes associated with antifungal drug resistance, including twenty previously described and five we identified as upregulated proteins following caspofungin exposure (Table 1): *i) CEK1* (CAGL0K04169g), *ii) CDC55* (CAGL0L06182g), *iii) CDC6* (CAGL0K00605g), *iv) DOT6* (CAGL0I05060g), *v) FKS1* (CAGL0G01034g), *vi) FKS2* (CAGL0K04037g), *vii) FKS3* (CAGL0M13827g), *viii) MKT1* (CAGL0J05566g), *ix) MOH1* (CAGL0F04631g), *x) MPH1* (CAGL0F04895g), *xi) MRPL11* (CAGL0J09724g), *xii) MSH2* (CAGL0I07733g), *xiii) PDR1* (CAGL0A00451g), *xiv) PHO4* (CAGL0D05170g), *xv) SNQ2* (CAGL0I04862g), *xvi) SUI2* (CAGL0B03795g), *xvii) TCB1* (CAGL0J08591g), *xviii) TCB3* (CAGL0L11440g), *xix) TOD6* (CAGL0A04257g), *xx) TPK2* (CAGL0M08404g), and *xxi) CRZ1* (CAGL0L00605g), *xxii) SLT2* (CAGL0J00539g), *xiii) SRP1* (CAGL0J11440g), *xiv) DBP5* (CAGL0L110021g), *xv) SWI1* (CAGL0C01683g). For each of these genes, multiple sequence alignment (nucleotide and amino acid) and mutation identification was performed using T-Coffee<sup>67</sup> and JalView<sup>65</sup> for visualization.

Computational transmembrane regions predictions were carried out using RaptorX<sup>68,69</sup>, Sable<sup>70–73</sup>, TMHMM v. 2.0<sup>74</sup>, TOPCONS<sup>75</sup>, TMpred<sup>76</sup>, CCTOP<sup>77,78</sup>, HMMTOP<sup>79</sup>, and Phobius<sup>80</sup>. InterProScan 5<sup>81</sup> was used for primary protein structure analysis.

### **Proteomic analysis**



Resistant CAGL1875 isolate was grown for 7h at 30°C with shaking in YPD and YPD with caspofungin (0,5 µg/mL), four biological replicates were performed to each condition. For viability assay, propidium iodide was made. Cell extracts were obtained suspending cells in lysis buffer (50 mM Tris-HCl pH 7.5, 1 mM EDTA, 150 mM NaCl, 1 mM DTT, 0.5 mM PMSF, and 10 % of a mix of protease inhibitors (Pierce TM)) and disrupted by centrifugation adding glass beads (0.4-0.6 mm diameter) in a Fast-Prep system (Bio101, Savant) applying five 20s rounds at 5.5 speed with intermediate ice cooling. Cell extracts were separated from glass beads by centrifugation and the supernatant was collected and cleared by centrifugation. Protein concentration was measured by Bradford protein assay. Digestion and desalting of peptides were carried out in gel with trypsin, according to Sechi and Chait<sup>82</sup>.

The desalted protein digest was analyzed by RP-LC-ESI-MS/MS in an EASY nLC 1000 System coupled to the Q-Exactive HF mass spectrometer through the Nano-Easy spray source (all from Thermo Scientific, Mississauga, ON, Canada). Peptide identification from raw data were carried out using Mascot v. 2.6.1 search engine through the Protein Discoverer 2.2 Software (Thermo Scientific). Database search was performed against SwissProt. Mascot Scores were adjusted by a percolator algorithm. The acceptance criteria for protein identification were an FDR < 1% and at least one peptide identified with high confidence (CI>95%). To determine the abundances of the identified peptides and proteins, a processing free label workflow was initiated in the first step. The recalibration of the masses was performed through a rapid search in Sequest HT against the database. Based on the positive identifications, an alignment of the chromatograms of all the samples with a tolerance of up to 10 min were established<sup>83,84</sup>.

Subsequently, alignment of the retention times between the different analyzed samples for the quantification of the precursor ions was performed, taking into account the unique peptides and the razor peptides (i.e., peptides that can be assigned to more than one protein). Finally, the results were normalized to the total amount of the peptides, equaling the total abundance among the different samples. After the analyses were finalized, a final report presented the list of peptide groups and proteins with scaled abundances and selected ratios. The Proteome Discoverer application includes a feature for assessing the significance of differential expression by providing p-values for those ratios (p-value <0.05). The mass spectrometry proteomics data have been deposited to the ProteomeXchange Consortium via the PRIDE<sup>85,86</sup> partner repository with the dataset identifier PXD021578 and 10.6019/PXD021578.

### **Antifungal susceptibility testing**

Antifungal susceptibility testing was carried out using the Clinical and Laboratory Standards Institute broth microdilution method (CLSI-BMD), following the M27-A3 guidelines with slight modifications for the combination of caspofungin with the calcineurin inhibitors<sup>87</sup>. Briefly, isolates were subcultured on yeast extract peptone dextrose agar (YPD) and grown for 24 h at 35 °C. The yeast suspensions were prepared in liquid RPMI 1640 medium (Sigma-Aldrich) to a final concentration of  $0.5 \times 10^3$  -  $2.5 \times 10^3$  cells/mL. Yeast inoculum (100- $\mu$ l) was added to a 96-well plate containing serial two-fold dilutions of caspofungin with or without inhibitors tacrolimus (Fk506) or cyclosporin A (CsA) (15  $\mu$ g/mL). MICs were visualized, and densitometry was determined as the lowest concentration of drug that caused a significant decrease (MIC-2 or  $\geq 50\%$ ) compared with that of the drug-free growth control after 48 h of incubation. Quality control was ensured by

400 testing the CLSI-recommended strains *C. parapsilosis* ATCC 22019 and *C. krusei* ATCC  
401 6258<sup>88</sup>.

## 402 **Stress-related phenotypic assays**

403 To examine the potential role of calcineurin in cellular protection of *C. glabrata* from heat  
404 and oxidative stresses, we assessed the impact of Fk506 and CsA, with or without  
405 caspofungin. For heat-shock stress, drop tests were performed by spotting serial dilutions of  
406 *C. glabrata* cells ( $10^6$  to  $10^3$  cells/mL) onto YPD agar plates with Fk506 or CsA (15  
407  $\mu\text{g/mL}$ ), caspofungin (1  $\mu\text{g/mL}$ ) or both compounds. The plates were incubated at 37°C or  
408 40°C for 24 h. For oxidative stress, YPD plates were prepared as previously except that the  
409 medium was supplemented with the naphtoquinone menadione (0.2 and 0.4 mM). The  
410 plates were incubated at 37°C for 24 h<sup>11,26</sup>.

## 411 **Biofilm formation**

412 The *C. glabrata* isolates were grown on Sabouraud medium (Biomérieux, France) and  
413 incubated at 30 °C for 24 h. Two hundred  $\mu\text{L}$  of *Candida* cell suspensions ( $10^6$  cells/mL) in  
414 RPMI-1640 with MOPS adjusted to pH 7 were seeded in 96-well microdilution wells with  
415 or without GDHK-1325 250mm Gam polyurethane catheter pieces (Hechingen, Germany)  
416 and allowed to adhere for 24 h at 37°C. The non-adherent cells were then removed by  
417 gently washing twice with 300  $\mu\text{L}$  PBS or by redisposing catheter pieces in new  
418 microplates wells. Caspofungin was added at 1  $\mu\text{g/mL}$  with and without 15  $\mu\text{g/mL}$  of the  
419 calcineurin inhibitors for 24 h incubation at 37 °C for biofilm adhesion phase. Then wells  
420 or catheter pieces were washed twice with PBS and finally 100 $\mu\text{L}$  of RPMI-1640 plus 10 $\mu\text{L}$   
421 of 700 $\mu\text{M}$  resazurin (Sigma-Aldrich) was added to each well and incubated at 37°C for 4 h.

<sup>89</sup>. Fluorescence was measured at 560nm with an emission at 590nm. The results are expressed in arbitrary fluorescence unit (AU).

#### **Invertebrate *Galleria mellonella* model**

Killing assays were performed in *G. mellonella* as described by Fallon, 2012 <sup>90</sup>. Briefly, the larvae were obtained from a Scientia breeding facility (Cali-Colombia); larvae of late stages (fifth and sixth) between 250 to 330 mg and a length of approximately 2 cm were selected. A group of 10 larvae was used for each of the controls: absolute control, disinfection, and inoculation. To compare mortality, three biological replicates were performed with 10 larvae for each isolate evaluated. The isolates were grown in Sabouraud dextrose agar and incubated for 48 hours at 35 °C. Suspensions adjusted to 1x10<sup>9</sup> UFC/mL using Neubauer chamber were used to inoculate 10 larvae per *Candida* isolate. Larvae receive 10µL of inoculum and caspofungin (1 µg/Larvae-100mg/L), Fk506 and CsA (15µg/mL), or their combination by injection into the last left and right proto-leg using a 0.5mL gauge insulin syringe. After inoculation, larvae were placed in Petri dishes and incubated in darkness at 37°C, the number of dead larvae was recorded daily.

#### **Statistical Analysis**

All experiments were performed on three independent biological replicates; survival curves were constructed using the method of Kaplan and Meier, then the curves were compared using the Log-Rank (Mantel-Cox) test. Statistical models were constructed and analyzed using PRISM software version 7.

#### **Data availability**

All experimental data are provided in the manuscript and in supplemental files, or available via ProteomeXchange with identifier PXD021578 (10.6019/PXD021578) and in the NCBI BioProject database with the accession number PRJNA648794.

## **Acknowledgements**

This study was financially supported by ECOS Nord C17S01, and the research vice rector of the Pontificia Universidad Javeriana in Bogotá, Colombia ID20291 and Colombian Science Technology and Innovation Department (Minciencias) Call 757. We thank Campus France (Eiffel scholarship) and the Complutense University of Madrid (member of ProteoRed-ISCI network). Finally, we thank Diego Vesga and Eduardo Romeu for their support in obtaining proteomic data.

## **Authors' contributions**

AC-G performed experiments and wrote the main manuscript, AC-G, LM, CG designed proteomic experiments and analyzed proteomic data, CA-M analyzed clinical implications, NEV-V conducted bioinformatics analysis of genomic data, and prepared figure 1, DME, JB isolates sequencing, AC, PLP, CP-G designed the experiments and wrote the final manuscript, and PLP, CP-G conceived the experiments and managed the resources. All authors have read and agreed to the published version of the manuscript.

## **Competing interest**

P.L.P received grants from Astellas, Basilea, MSD and Pfizer and speaker's fees from Gilead, Basilea, Pfizer and MSD. The other authors declare no conflict of interest.

## **References**

- 464 1. Pappas, P. G. *et al.* Clinical Practice Guideline for the Management of Candidiasis:  
465 2016 Update by the Infectious Diseases Society of America. *Clin. Infect. Dis.* **62**,  
466 civ933 (2015).
- 467 2. Oñate, J. M. *et al.* Colombian consensus on the diagnosis, treatment, and prevention  
468 of Candida Spp. disease in children and adults\*,+. *Infectio* **23**, 271 (2019).
- 469 3. Perlin, D. S. Echinocandin Resistance in Candida. *Clin. Infect. Dis.* **61 Suppl 6**,  
470 S612-7 (2015).
- 471 4. Healey, K. & Perlin, D. Fungal Resistance to Echinocandins and the MDR  
472 Phenomenon in Candida glabrata. *J. Fungi* 2018, Vol. 4, Page 105 **4**, 105 (2018).
- 473 5. Garcia-Effron, G., Park, S. & Perlin, D. S. Correlating Echinocandin MIC and  
474 Kinetic Inhibition of fks1 Mutant Glucan Synthases for Candida albicans:  
475 Implications for Interpretive Breakpoints. *Antimicrob. Agents Chemother.* **53**, 112–  
476 122 (2009).
- 477 6. Garcia-Effron, G., Lee, S., Park, S., Cleary, J. D. & Perlin, D. S. Effect of Candida  
478 glabrata FKS1 and FKS2 mutations on echinocandin sensitivity and kinetics of 1,3-  
479 beta-D-glucan synthase: implication for the existing susceptibility breakpoint.  
480 *Antimicrob. Agents Chemother.* **53**, 3690–9 (2009).
- 481 7. Katiyar, S. K. *et al.* Fks1 and Fks2 are functionally redundant but differentially  
482 regulated in Candida glabrata: implications for echinocandin resistance. *Antimicrob.*  
483 *Agents Chemother.* **56**, 6304–6309 (2012).
- 484 8. Garcia-Effron, G., Katiyar, S. K., Park, S., Edlind, T. D. & Perlin, D. S. A Naturally  
485 Occurring Proline-to-Alanine Amino Acid Change in Fks1p in Candida parapsilosis,  
486 Candida orthopsilosis, and Candida metapsilosis Accounts for Reduced  
487 Echinocandin Susceptibility. *Antimicrob. Agents Chemother.* **52**, 2305–2312 (2008).
- 488 9. Singh-Babak, S. D. *et al.* Global Analysis of the Evolution and Mechanism of  
489 Echinocandin Resistance in Candida glabrata. *PLoS Pathog.* **8**, e1002718 (2012).
- 490 10. Cowen, L. E. & Steinbach, W. J. Stress, Drugs, and Evolution: the Role of Cellular  
491 Signaling in Fungal Drug Resistance. *Eukaryot. Cell* **7**, 747–764 (2008).
- 492 11. Ceballos Garzon, A., Amado, D., Robert, E., Parra Giraldo, C. M. & Le Pape, P.  
493 Impact of calmodulin inhibition by fluphenazine on susceptibility, biofilm formation  
494 and pathogenicity of caspofungin-resistant Candida glabrata. *J. Antimicrob.*  
495 *Chemother.* **75**, 1187–1193 (2020).
- 496 12. Shapiro, R. S., Robbins, N. & Cowen, L. E. Regulatory circuitry governing fungal  
497 development, drug resistance, and disease. *Microbiol. Mol. Biol. Rev.* **75**, 213–267  
498 (2011).
- 499 13. LaFayette, S. L. *et al.* PKC signaling regulates drug resistance of the fungal  
500 pathogen Candida albicans via circuitry comprised of Mkc1, calcineurin, and Hsp90.  
501 *PLoS Pathog.* **6**, e1001069 (2010).
- 502 14. Reinoso-Martín, C., Schüller, C., Schuetzer-Muehlbauer, M. & Kuchler, K. The

- 503 yeast protein kinase C cell integrity pathway mediates tolerance to the antifungal  
504 drug caspofungin through activation of Slt2p mitogen-activated protein kinase  
505 signaling. *Eukaryot. Cell* **2**, 1200–10 (2003).
- 506 15. Chen, Y.-L. *et al.* Calcineurin Controls Drug Tolerance, Hyphal Growth, and  
507 Virulence in *Candida dubliniensis*. *Eukaryot. Cell* **10**, 803–819 (2011).
- 508 16. Onyewu, C., Wormley, F. L., Perfect, J. R. & Heitman, J. The Calcineurin Target,  
509 Crz1, Functions in Azole Tolerance but Is Not Required for Virulence of *Candida*  
510 *albicans*. *Infect. Immun.* **72**, 7330–7333 (2004).
- 511 17. Miyazaki, T. *et al.* Functional characterization of the regulators of calcineurin in  
512 *Candida glabrata*. *FEMS Yeast Res.* **11**, 621–630 (2011).
- 513 18. Juvvadi, P. R., Lee, S. C., Heitman, J. & Steinbach, W. J. Calcineurin in fungal  
514 virulence and drug resistance: Prospects for harnessing targeted inhibition of  
515 calcineurin for an antifungal therapeutic approach. *Virulence* **8**, 186–197 (2016).
- 516 19. Beom, J. Y. *et al.* Biosynthesis of Nonimmunosuppressive FK506 Analogues with  
517 Antifungal Activity. *J. Nat. Prod.* **82**, 2078–2086 (2019).
- 518 20. Breuder, T., Hemenway, C. S., Movva, N. R., Cardenas, M. E. & Heitman, J.  
519 Calcineurin is essential in cyclosporin A- and FK506-sensitive yeast strains. *Proc.*  
520 *Natl. Acad. Sci. U. S. A.* **91**, 5372–5376 (1994).
- 521 21. Hoehamer, C. F., Cummings, E. D., Hilliard, G. M. & Rogers, P. D. Changes in the  
522 proteome of *Candida albicans* in response to azole, polyene, and echinocandin  
523 antifungal agents. *Antimicrob. Agents Chemother.* (2010) doi:10.1128/AAC.00756-  
524 09.
- 525 22. Bruneau, J. M. *et al.* Drug induced proteome changes in *Candida albicans*:  
526 Comparison of the effect of  $\beta(1,3)$  glucan synthase inhibitors and two triazoles,  
527 fluconazole and itraconazole. *Proteomics* **3**, 325–336 (2003).
- 528 23. Fernández-Arenas, E. *et al.* Integrated proteomics and genomics strategies bring new  
529 insight into *Candida albicans* response upon macrophage interaction. *Mol. Cell.*  
530 *Proteomics* **6**, 460–478 (2007).
- 531 24. Vaz, C. *et al.* Enrichment of ATP Binding Proteins Unveils Proteomic Alterations in  
532 Human Macrophage Cell Death, Inflammatory Response, and Protein Synthesis after  
533 Interaction with *Candida albicans*. *J. Proteome Res.* **18**, 2139–2159 (2019).
- 534 25. Reales-Calderón, J. A., Vaz, C., Monteoliva, L., Molero, G. & Gil, C. *Candida*  
535 *albicans* Modifies the Protein Composition and Size Distribution of THP-1  
536 Macrophage-Derived Extracellular Vesicles. *J. Proteome Res.* **16**, 87–105 (2017).
- 537 26. Gil-Bona, A. *et al.* The Cell Wall Protein Ecm33 of *Candida albicans* is Involved in  
538 Chronological Life Span, Morphogenesis, Cell Wall Regeneration, Stress Tolerance,  
539 and Host-Cell Interaction. *Front. Microbiol.* **7**, 64 (2016).
- 540 27. O’Meara, T. R. *et al.* Global proteomic analyses define an environmentally  
541 contingent Hsp90 interactome and reveal chaperone-dependent regulation of stress

542 granule proteins and the R2TP complex in a fungal pathogen. *PLOS Biol.* **17**, 1–38  
543 (2019).

544 28. Jayampath Seneviratne, C., Wang, Y., Jin, L., Abiko, Y. & Samaranayake, L. P.  
545 Proteomics of drug resistance in candida glabrata biofilms. *Proteomics* **10**, 1444–  
546 1454 (2010).

547 29. Gómez-Molero, E. *et al.* Proteomic analysis of hyperadhesive Candida glabrata  
548 clinical isolates reveals a core wall proteome and differential incorporation of  
549 adhesins. *FEMS Yeast Res.* **15**, 1–10 (2015).

550 30. Pais, P. *et al.* Membrane proteome-wide response to the antifungal drug clotrimazole  
551 in Candida glabrata: Role of the transcription factor CgPdr1 and the Drug:H+  
552 antiporters CgTpo1-1 and CgTpo1-2. *Mol. Cell. Proteomics* **15**, 57–72 (2016).

553 31. Pais, P. *et al.* Membrane Proteomics Analysis of the Candida glabrata Response to 5-  
554 Flucytosine: Unveiling the Role and Regulation of the Drug Efflux Transporters  
555 CgFlr1 and CgFlr2. *Front. Microbiol.* **7**, 2045 (2016).

556 32. Diekema, D., Arbefeville, S., Boyken, L., Kroeger, J. & Pfaller, M. The changing  
557 epidemiology of healthcare-associated candidemia over three decades. *Diagn.*  
558 *Microbiol. Infect. Dis.* **73**, 45–48 (2012).

559 33. Kumar, K., Askari, F., Sahu, M. S. & Kaur, R. Candida glabrata: A lot more than  
560 meets the eye. *Microorganisms* vol. 7 39 (2019).

561 34. Toda, M. *et al.* Population-Based Active Surveillance for Culture-Confirmed  
562 Candidemia — Four Sites, United States, 2012–2016. *MMWR. Surveill. Summ.* **68**,  
563 1–15 (2019).

564 35. Whaley, S. G. & Rogers, P. D. Azole Resistance in Candida glabrata. *Current*  
565 *Infectious Disease Reports* vol. 18 1–10 (2016).

566 36. Alexander, B. D. *et al.* Increasing Echinocandin Resistance in Candida glabrata:  
567 Clinical Failure Correlates With Presence of FKS Mutations and Elevated Minimum  
568 Inhibitory Concentrations. *Clin Infect Dis* . **56**, 1724–1732 (2013).

569 37. Zimbeck, A. J. *et al.* FKS Mutations and Elevated Echinocandin MIC Values among  
570 Candida glabrata Isolates from U.S. Population-Based Surveillance. *Antimicrob.*  
571 *Agents Chemother.* **54**, 5042–5047 (2010).

572 38. Yu, S. J., Chang, Y. L. & Chen, Y. L. Calcineurin signaling: Lessons from Candida  
573 species. *FEMS Yeast Res.* **15**, 1–7 (2015).

574 39. Denning, D. W. Echinocandin antifungal drugs. *Lancet (London, England)* **362**,  
575 1142–51 (2003).

576 40. Kelly, J. & Kavanagh, K. Proteomic analysis of proteins released from growth-  
577 arrested Candida albicans following exposure to caspofungin. *Med. Mycol.* **48**, 598–  
578 605 (2010).

579 41. Román, E., Alonso-Monge, R., Miranda, A. & Pla, J. The Mkk2 MAPKK Regulates  
580 Cell Wall Biogenesis in Cooperation with the Cek1-Pathway in Candida albicans.



581 *PLoS One* **10**, e0133476 (2015).

582 42. Alonso-Monge, R. *et al.* The Fungicidal Action of Micafungin is Independent on  
583 Both Oxidative Stress Generation and HOG Pathway Signaling in *Candida albicans*.  
584 *Microorganisms* **8**, 1867 (2020).

585 43. Singh, S. D. *et al.* Hsp90 governs echinocandin resistance in the pathogenic yeast  
586 *Candida albicans* via calcineurin. *PLoS Pathog.* **5**, e1000532 (2009).

587 44. Miyazaki, T. *et al.* Role of the Slt2 mitogen-activated protein kinase pathway in cell  
588 wall integrity and virulence in *Candida glabrata*. *FEMS Yeast Res.* (2010)  
589 doi:10.1111/j.1567-1364.2010.00611.x.

590 45. Vasicova, P., Stradalova, V., Halada, P., Hasek, J. & Malcova, I. Nuclear Import of  
591 Chromatin Remodeler Isw1 Is Mediated by Atypical Bipartite cNLS and Classical  
592 Import Pathway. *Traffic* **14**, 176–193 (2013).

593 46. Tieg, B. & Krebber, H. Dbp5 - From nuclear export to translation. *Biochim. Biophys.*  
594 *Acta* **1829**, 791–799 (2013).

595 47. Ha, S. W., Ju, D. & Xie, Y. Nuclear import factor Srp1 and its associated protein  
596 Sts1 couple ribosome-bound nascent polypeptides to proteasomes for cotranslational  
597 degradation. *J. Biol. Chem.* (2014) doi:10.1074/jbc.M113.524926.

598 48. Chen, L. & Madura, K. Yeast Importin- $\alpha$  (Srp1) performs distinct roles in the import  
599 of nuclear proteins and in targeting proteasomes to the nucleus. *J. Biol. Chem.*  
600 (2014) doi:10.1074/jbc.M114.582023.

601 49. Mazáň, M., Mazáňová, K. & Farkaš, V. Phenotype analysis of *Saccharomyces*  
602 *cerevisiae* mutants with deletions in Pir cell wall glycoproteins. *Antonie van*  
603 *Leeuwenhoek, Int. J. Gen. Mol. Microbiol.* **94**, 335–42 (2008).

604 50. De Groot, P. W. J. *et al.* The cell wall of the human pathogen *Candida glabrata*:  
605 Differential incorporation of novel adhesin-like wall proteins. *Eukaryot. Cell* **7**,  
606 1951–1964 (2008).

607 51. Kandasamy, R., Vedyappan, G. & Chaffin, W. L. Evidence for the presence of Pir-  
608 like proteins in *Candida albicans*. *FEMS Microbiol. Lett.* **186**, 239–43 (2000).

609 52. Walker, L. A., Gow, N. A. R. & Munro, C. A. Elevated Chitin Content Reduces the  
610 Susceptibility of *Candida* Species to Caspofungin. *Antimicrob. Agents Chemother.*  
611 **57**, 146–154 (2013).

612 53. Walker, L. A. & Munro, C. A. Caspofungin Induced Cell Wall Changes of *Candida*  
613 Species Influences Macrophage Interactions. *Front. Cell. Infect. Microbiol.* **10**, 164  
614 (2020).

615 54. Chen, Y.-L. *et al.* Convergent Evolution of Calcineurin Pathway Roles in  
616 Thermotolerance and Virulence in *Candida glabrata*. *G3 Genes, Genomes, Genet.* **2**,  
617 675–691 (2012).

618 55. Cuéllar-Cruz, M. *et al.* High Resistance to Oxidative Stress in the Fungal Pathogen  
619 *Candida glabrata* Is Mediated by a Single Catalase, Cta1p, and Is Controlled by the

620 Transcription Factors Yap1p, Skn7p, Msn2p, and Msn4p. *Eukaryot. Cell* **7**, 814–825  
621 (2008).

622 56. Fonseca, E. *et al.* Effects of fluconazole on *Candida glabrata* biofilms and its  
623 relationship with ABC transporter gene expression. *Biofouling* **30**, 447–457 (2014).

624 57. Rodrigues, C. F., Rodrigues, M. E. & Henriques, M. Susceptibility of *Candida*  
625 *glabrata* biofilms to echinocandins: alterations in the matrix composition. *Biofouling*  
626 **34**, 569–578 (2018).

627 58. Park, H.-S. *et al.* Calcineurin Targets Involved in Stress Survival and Fungal  
628 Virulence. *PLOS Pathog.* **12**, e1005873 (2016).

629 59. Bashir, Q., LeMaster, D. M. & Hernández, G. 1H, 13C, 15 N chemical shift  
630 assignments of the FKBP12 protein from the pathogenic fungi *Candida auris* and  
631 *Candida glabrata*. *Biomol. NMR Assign.* **14**, 105–109 (2020).

632 60. Lee, Y. *et al.* In vitro and in vivo assessment of FK506 analogs as novel antifungal  
633 drug candidates. *Antimicrob. Agents Chemother.* **62**, e01627-18 (2018).

634 61. Malik, A. *et al.* Molecular docking and pharmacokinetic evaluation of natural  
635 compounds as targeted inhibitors against Crz1 protein in *Rhizoctonia solani*.  
636 *Bioinformation* **15**, 277–286 (2019).

637 62. Bahn, Y.-S. Exploiting Fungal Virulence-Regulating Transcription Factors As Novel  
638 Antifungal Drug Targets. *PLOS Pathog.* **11**, e1004936 (2015).

639 63. Chen, S., Zhou, Y., Chen, Y. & Gu, J. fastp: an ultra-fast all-in-one FASTQ  
640 preprocessor. *Bioinformatics* **34**, i884–i890 (2018).

641 64. Bankevich, A. *et al.* SPAdes: A New Genome Assembly Algorithm and Its  
642 Applications to Single-Cell Sequencing. *J. Comput. Biol.* **19**, 455 (2012).

643 65. Waterhouse, A. M., Procter, J. B., Martin, D. M. A., Clamp, M. & Barton, G. J.  
644 Jalview Version 2--a multiple sequence alignment editor and analysis workbench.  
645 *Bioinformatics* **25**, 1189–1191 (2009).

646 66. Altschul, S. F., Gish, W., Miller, W., Myers, E. W. & Lipman, D. J. Basic local  
647 alignment search tool. *J. Mol. Biol.* **215**, 403–410 (1990).

648 67. Notredame, C., Higgins, D. G. & Heringa, J. T-coffee: a novel method for fast and  
649 accurate multiple sequence alignment 1 Edited by J. Thornton. *J. Mol. Biol.* **302**,  
650 205–217 (2000).

651 68. Källberg, M. *et al.* Template-based protein structure modeling using the RaptorX  
652 web server. *Nat. Protoc.* **7**, 1511–1522 (2012).

653 69. Wang, Z., Zhao, F., Peng, J. & Xu, J. Protein 8-class secondary structure prediction  
654 using conditional neural fields. *Proteomics* **11**, 3786–3792 (2011).

655 70. Adamczak, R., Porollo, A. & Meller, J. Accurate prediction of solvent accessibility  
656 using neural networks-based regression. *Proteins Struct. Funct. Bioinforma.* **56**,  
657 753–767 (2004).

- 658 71. Adamczak, R., Porollo, A. & Meller, J. Combining prediction of secondary structure  
659 and solvent accessibility in proteins. *Proteins Struct. Funct. Bioinforma.* **59**, 467–  
660 475 (2005).
- 661 72. Wagner, M., Adamczak, R., Porollo, A. & Meller, J. Linear Regression Models for  
662 Solvent Accessibility Prediction in Proteins. *J. Comput. Biol.* **12**, 355–369 (2005).
- 663 73. Porollo, A., Adamczak, R., Wagner, M. & Meller, J. Maximum Feasibility Approach  
664 for Consensus Classifiers: Applications to Protein Structure Prediction. 1–6  
665 [https://folding.cchmc.org/publications/ciras2003\\_jmeller.pdf](https://folding.cchmc.org/publications/ciras2003_jmeller.pdf) (2004).
- 666 74. Krogh, A., Larsson, B., von Heijne, G. & Sonnhammer, E. L. . Predicting  
667 transmembrane protein topology with a hidden markov model: application to  
668 complete genomes | Edited by F. Cohen. *J. Mol. Biol.* **305**, 567–580 (2001).
- 669 75. Tsirigos, K. D., Peters, C., Shu, N., Käll, L. & Elofsson, A. The TOPCONS web  
670 server for consensus prediction of membrane protein topology and signal peptides.  
671 *Nucleic Acids Res.* **43**, W401–W407 (2015).
- 672 76. K, H. & W, S. A database of membrane spanning proteins segments. *Biol. Chem.*  
673 *Hoppe-Seyler.* **374**, (1993).
- 674 77. Dobson, L., Reményi, I. & Tusnády, G. E. CCTOP: a Consensus Constrained  
675 TOPology prediction web server. *Nucleic Acids Res.* **43**, W408 (2015).
- 676 78. Dobson, L., Reményi, I. & Tusnády, G. E. The human transmembrane proteome.  
677 *Biol. Direct* **10**, (2015).
- 678 79. Tusnady, G. E. & Simon, I. The HMMTOP transmembrane topology prediction  
679 server. *Bioinformatics* **17**, 849–850 (2001).
- 680 80. Käll, L., Krogh, A. & Sonnhammer, E. L. . A Combined Transmembrane Topology  
681 and Signal Peptide Prediction Method. *J. Mol. Biol.* **338**, 1027–1036 (2004).
- 682 81. Jones, P. *et al.* InterProScan 5: genome-scale protein function classification.  
683 *Bioinformatics* **30**, 1236 (2014).
- 684 82. Sechi, S. & Chait, B. T. Modification of Cysteine Residues by Alkylation. A Tool in  
685 Peptide Mapping and Protein Identification. *Anal. Chem.* **70**, 5150–5158 (1998).
- 686 83. Brosch, M., Yu, L., Hubbard, T. & Choudhary, J. Accurate and sensitive peptide  
687 identification with mascot percolator. *J. Proteome Res.* **8**, 3176–3181 (2009).
- 688 84. Perkins, D. N., Pappin, D. J. C., Creasy, D. M. & Cottrell, J. S. Probability-based  
689 protein identification by searching sequence databases using mass spectrometry data.  
690 in *Electrophoresis* vol. 20 3551–3567 (Wiley-VCH Verlag, 1999).
- 691 85. Perez-Riverol, Y. *et al.* The PRIDE database and related tools and resources in 2019:  
692 Improving support for quantification data. *Nucleic Acids Res.* **47**, D442–D450  
693 (2019).
- 694 86. Deutsch, E. W. *et al.* The ProteomeXchange consortium in 2020: Enabling ‘big data’  
695 approaches in proteomics. *Nucleic Acids Res.* **48**, D1145–D1152 (2020).

87. Clinical and Laboratory Standards Institute. Reference Method for Broth Dilution Antifungal Susceptibility Testing of Yeasts; Third Informational Supplement. CLSI Document M27-S3, Clinical and Laboratory Standards Institute, Wayne, Penn, USA. (2008).
88. CLSI. M27-S4 Reference Method for Broth Dilution Antifungal Susceptibility Testing of Yeasts; Fourth Informational Supplement An informational supplement for global application developed through the Clinical and Laboratory Standards Institute. (2012).
89. Le Pape, P., Pagniez, F. & Abdala-Valencia, H. A new fluorometric method for anti-Leishmania drug screening on axenic amastigotes. *Acta Parasitol.* **48**, 301–305 (2003).
90. Fallon, J., Kelly, J. & Kavanagh, K. *Galleria mellonella* as a Model for Fungal Pathogenicity Testing. *Methods Mol. Biol.* **845**, 469–85 (2012).
91. Omasits, U., Ahrens, C. H., Müller, S. & Wollscheid, B. Protter: interactive protein feature visualization and integration with experimental proteomic data. *Bioinformatics* **30**, 884–886 (2014).

## Tables and figures

**Table 1.** Genes associated with caspofungin resistance.

**Figure 1.** Multiple alignment of Fks2 (Beta-1,3-glucan synthase catalytic subunit 2) nucleotide and amino acid sequences among *C. glabrata* resistant and susceptible strains. Multiple nucleotide (A) and amino acid sequence alignments (B) that show a 3-nucleotide deletion (1974-CTT-1976) and a single amino acid deletion (F659-Del), respectively, occurring only in *C. glabrata* resistant strains. C.) A consensus *C. glabrata* Fks2 membrane protein structure and topology model predicted by seven different membrane protein secondary structure prediction servers and visualized with Protter<sup>91</sup>; hot spots 1 and 2 are showed in red, as well the position F659 in which occurs the single amino acid deletion associated with echinocandins resistance.

**Figure 2.** Label-free quantitative proteomics results. (A) Gene Ontology (GO) analysis of the proteins considered differentially abundant after caspofungine treatment. (M) molecular function and (P) biological process. The X-axis indicates the number of associated proteins (B) Protein abundance profile. Inside the brackets *Candida albicans* Orthologues names. Down-regulated proteins are marked green and up-regulated are marked red.

**Figure 3.** Analysis of proteins identified in caspofungin condition (A). Gene Ontology (GO) analysis of all the proteins whose abundance was modified after caspofungin treatment., MF (molecular function) and BP (biological process) (-) (B) Word enrichment that was created using the P-values and the full terms from the enrichment analysis via a program called GO summaries available at the FungiDB website: <https://fungidb.org/fungidb/app/> (C) STRING protein-protein interaction diagram constructed with proteins of interest found more abundant after caspofungin exposure (confidence score 0.400, STRING V.11) \* indicate the proteins predicted by STRING software. Filled protein nodes that signify the availability of protein 3D structural information is known or predicted

**Figure 4.** Caspofungin minimal inhibitory concentrations under basal and calcineurin inhibition. Resistant strains > 0.5 µg/mL (1875 and 1256).

**Figure 5.** Stress responses under CaM/Cal inhibition. (A) Strains were grown in the presence of 0.2 and 0.4 mM menadione (Med) (B) Heat shocked at 37°C and 40°C, with or without 1 µg/mL caspofungin (Cas) with or without 15 µg/mL Fk506, CsA. YPD\* at 37°C, free of the drug was considered as growth control

**Figure 6.** Biofilm formation of *C. glabrata* isolates in microplate wells (A) and on catheter pieces (B), exposed to CsA, FK506, caspofungin and their combinations. The data are expressed as arbitrary fluorescence unit.

**Figure 7.** *Galleria* time-kill curves of caspofungin-susceptible (A, B) and resistant (C, D) *C. glabrata* isolates exposed to, caspofungin, calcineurin inhibitors and their combinations. The data are expressed as the percentages of survival. Log-rank (Mantel–Cox) test with p-values of < 0.05 was used to indicate statistical significance. As follows, p < 0.05\* p < 0.02\*\* and p < 0.001\*\*\*.

## Supplementary

**Table S1.** Total identified proteins.

**Table S2.** Description of the differentially abundant proteins after caspofungin treatment.

**Table S3.** Description and analysis of the proteins identified in YPD or CAS conditions.

**Table 1.** Genes associated with caspofungin resistance.

Gene Symbol	Systematic name	Mutations	Mutation in resistant strains (1875-1256)	Resistance-associated mutation (+/-)
<i>CEK1</i>	CAGL0K04169g	-	-	-
<i>CDC55</i>	CAGL0L06182g	-	-	-
<i>CDC6</i>	CAGL0K00605g	R117K, V163A, K268R, R80K	-	-
<i>DOT6</i>	CAGL0I05060g	P104S	-	-
<i>FKS1</i>	CAGL0G01034g	G14S	-	-
<i>FKS2</i>	CAGL0K04037g	<b>F659-Del</b> , T926P	<b>F659-Del</b>	+
<i>FKS3</i>	CAGL0M13827g	A42V, T1676S	-	-
<i>MKT1</i>	CAGL0J05566g	N512K, A643T	-	-
<i>MOH1</i>	CAGL0F04631g	S15N	-	-
<i>MPH1</i>	CAGL0F04895g	-	-	-
<i>MRPL11</i>	CAGL0J09724g	-	-	-
<i>MSH2</i>	CAGL0I07733g	-	-	-
<i>PDR1</i>	CAGL0A00451g	V91I, L98S, D243N	-	-
<i>PHO4</i>	CAGL0D05170g	S327N	-	-
<i>SNQ2</i>	CAGL0I04862g	P1104H	-	-
<i>SUI2</i>	CAGL0B03795g	-	-	-
<i>TCB1</i>	CAGL0J08591g	Q437E, K585R, N622K	-	-
<i>TCB3</i>	CAGL0L11440g	-	-	-
<i>TOD6</i>	CAGL0A04257g	P64S, D81N, N85D	-	-
<i>TPK2</i>	CAGL0M08404g	T132A, T158A	-	-
<i>CRZ1</i> *	CAGL0M06831g	-	-	-
<i>SLT2</i> *	CAGL0J00539g	-	-	-
<i>SRP1</i> *	CAGL0J11440g	-	-	-
<i>DBP5</i> *	CAGL0L110021g	-	-	-
<i>SWI1</i> *	CAGL0C01683g	-	-	-

\* Genes of proteins found in this study

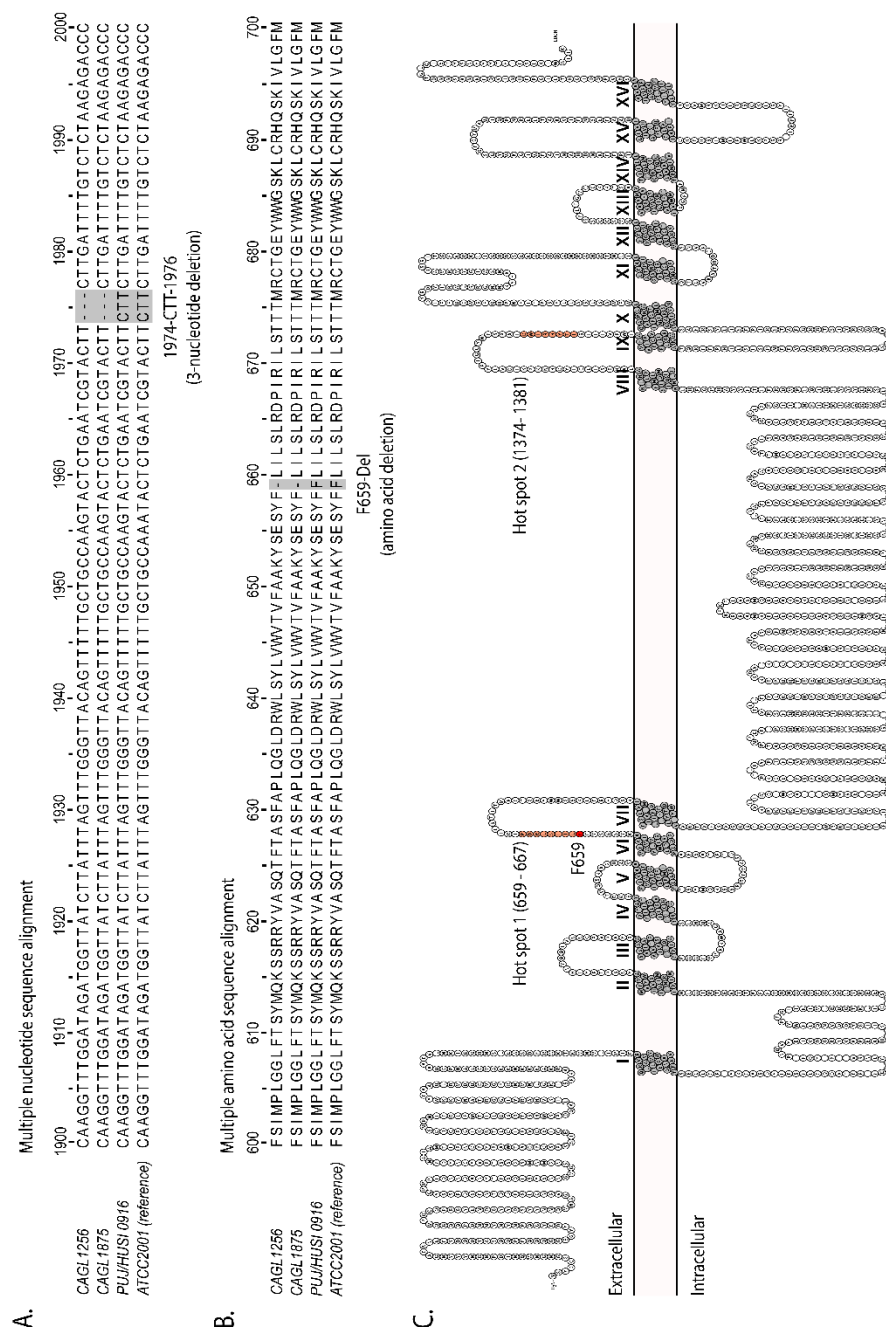


**Figure 1.** Multiple alignments of Fks2 (Beta-1,3-glucan synthase catalytic subunit 2) nucleotide and amino acid sequences from *C. glabrata* resistant and susceptible strains. Multiple nucleotide (A) and amino acid sequence alignments (B) that show a 3-nucleotide deletion (1974-CTT-1976) and a single amino acid deletion (F659-Del), respectively, occurring only in *C. glabrata* resistant strains. (C) A consensus *C. glabrata* Fks2 membrane protein structure and topology model predicted by seven different membrane protein secondary structure prediction servers and visualized with Protter<sup>91</sup>. Hot spots 1 and 2 are showed in red, as well the position F659 in which occurs the single amino acid deletion associated with echinocandins resistance.

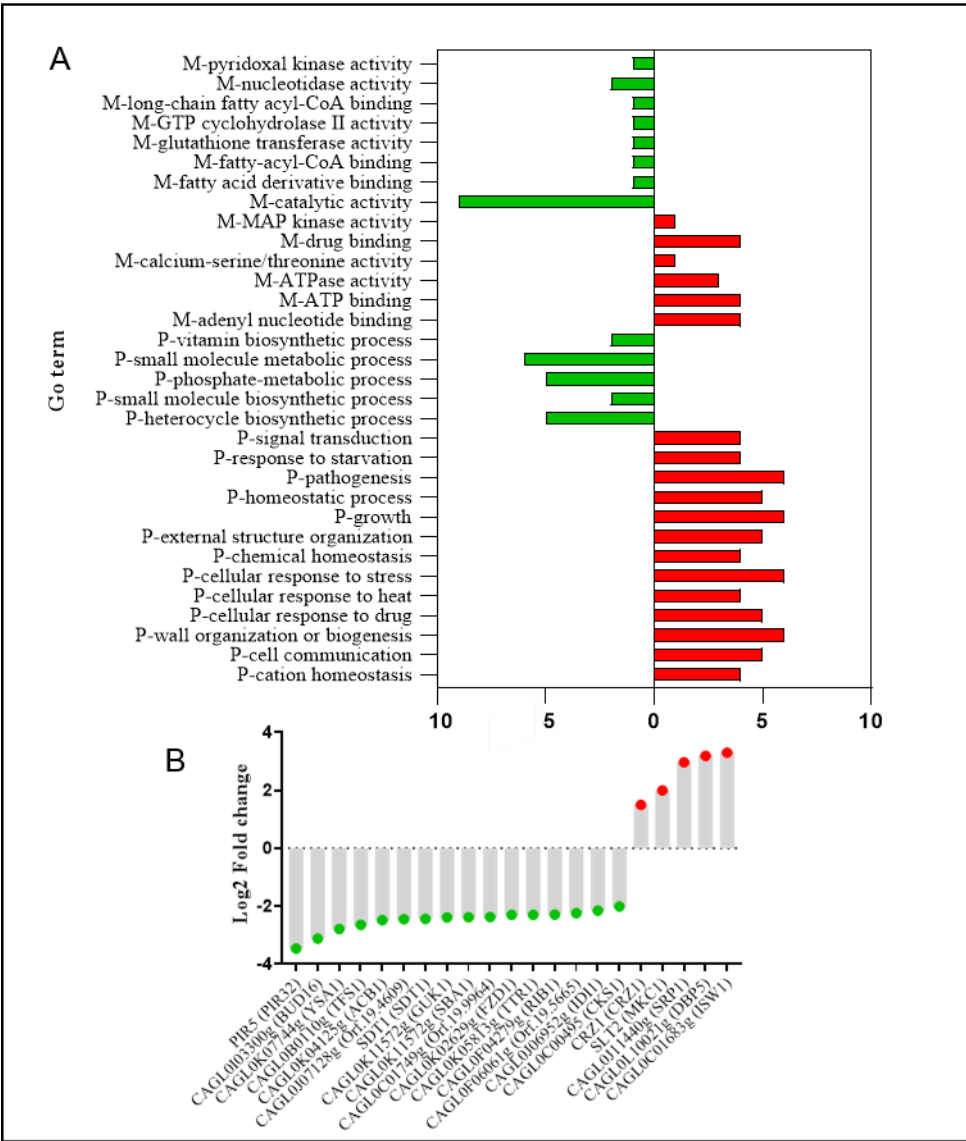


**Figure 2.** Label-free quantitative proteomics results. **(A)** Gene Ontology (GO) analysis of the proteins considered differentially abundant after caspofungine treatment. M = molecular function; P = biological process; X-axis indicates the number of associated proteins. **(B)** Protein abundance profile. Down-regulated proteins are marked green and up-regulated are marked red (*Candida albicans* orthologue names are inside the parantheses).



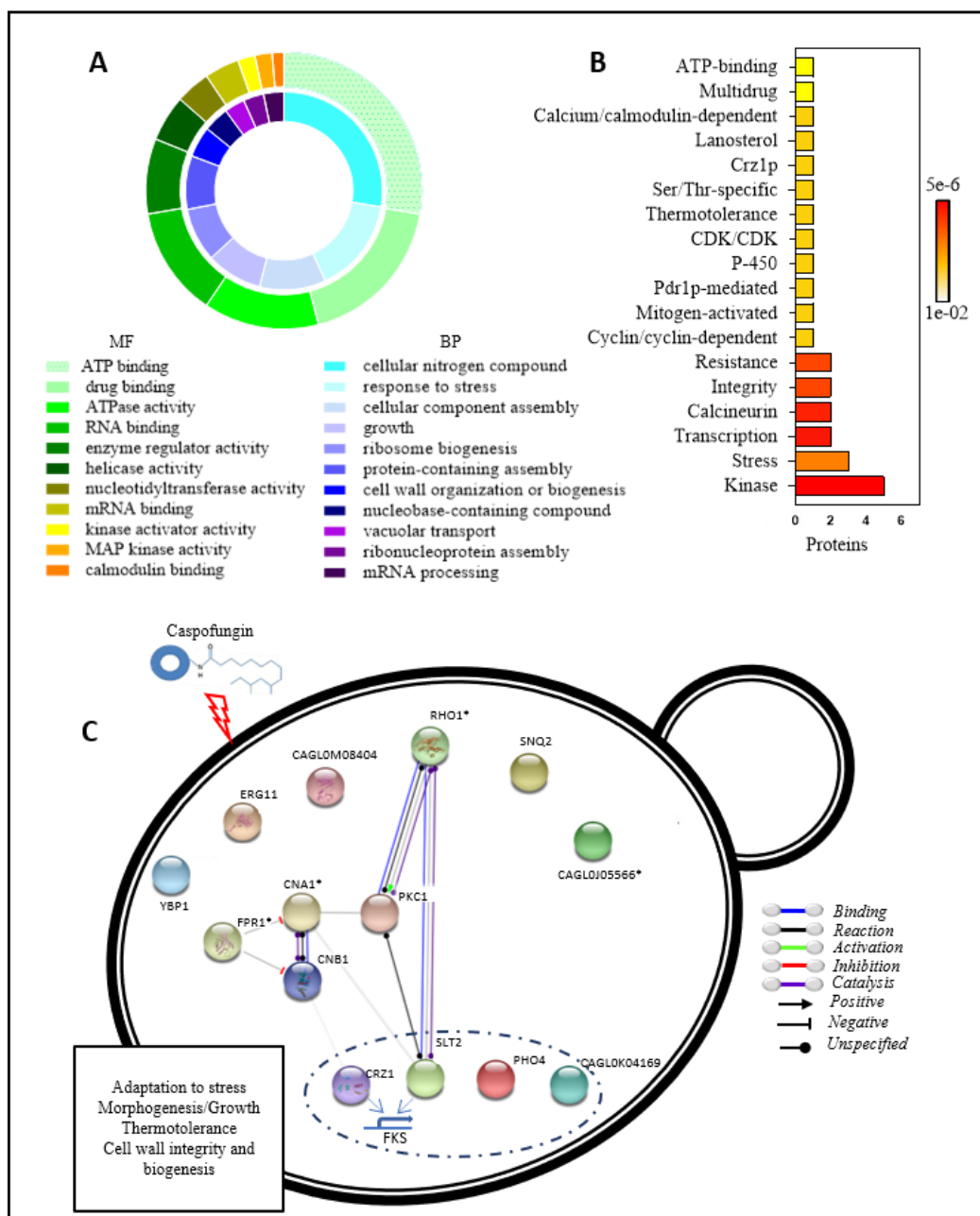


**Figure 3.** Analysis of proteins identified in caspofungin condition (A). Gene Ontology (GO) analysis of all the proteins whose abundance was modified after caspofungin treatment. MF = molecular function and BP = biological process. (B) GO Summary word enrichment created using the P-values and the full terms from the enrichment analysis. (C) STRING protein-protein interaction diagram constructed with upregulated proteins following caspofungin exposure (confidence score 0.400, STRING V.11). \* indicate the proteins predicted by STRING software. Filled protein nodes signify the availability of known or predicted protein 3D structural information.

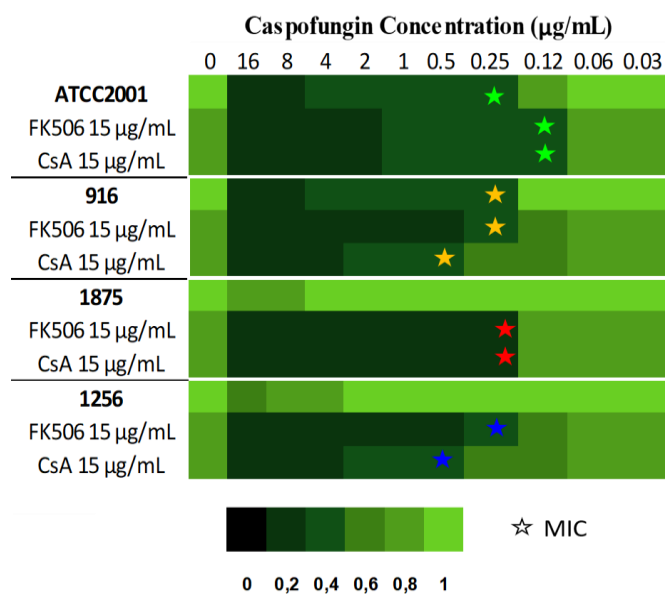


**Figure 4.** Caspofungin minimal inhibitory concentrations under basal and calcineurin inhibition, resistant strains > 0.5 µg/mL (1875 and 1256).

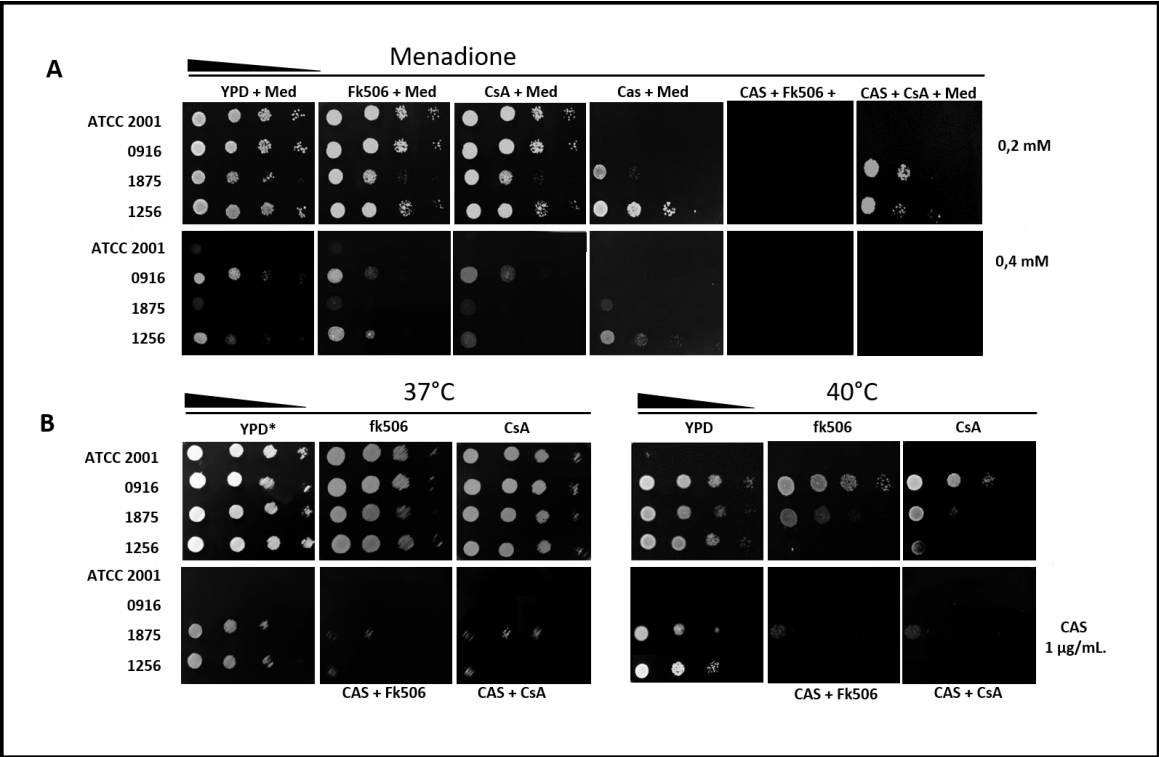


**Figure 5.** Stress responses under CaM/Cal inhibition. (A) Strains grown in the presence of 0.2 and 0.4 mM menadione (Med). (B) Strains heat shocked at 37°C and 40°C, with or without 1 µg/mL caspofungin (CAS), with or without 15 µg/mL Fk506, CsA. \*YPD at 37°C was used as no drug growth control.

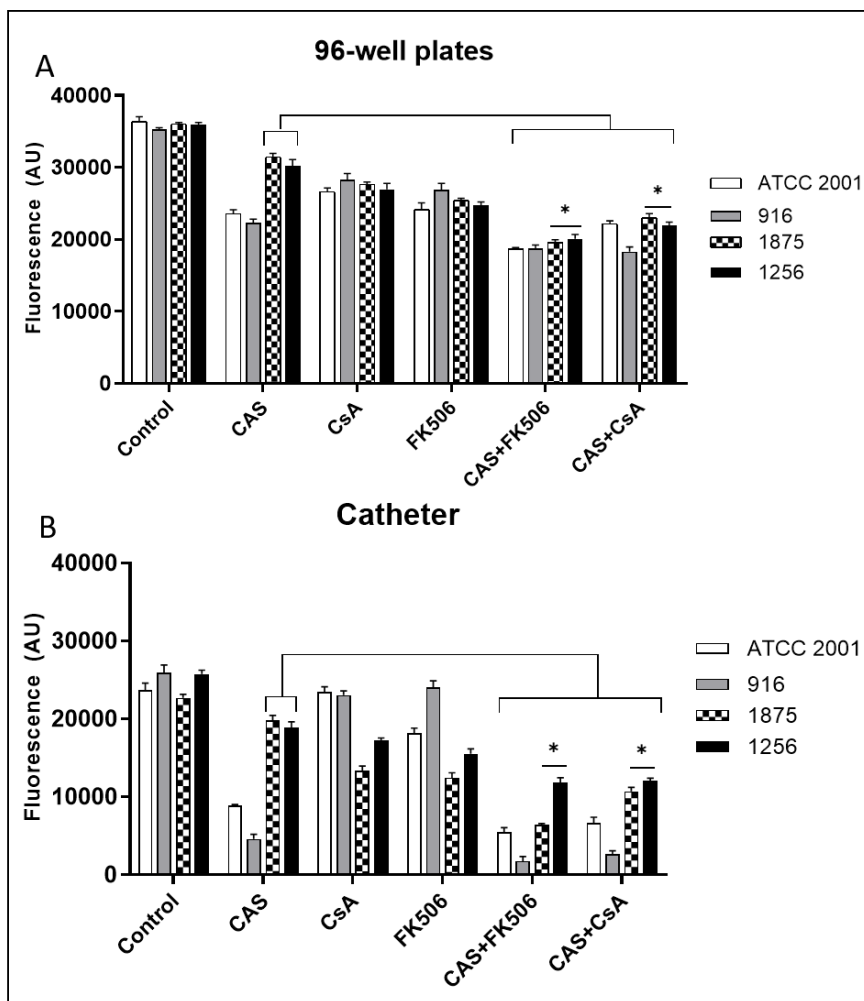


**Figure 6.** Biofilm formation of *C. glabrata* isolates grown (A) in microplate wells and (B) on catheter pieces; exposed to CsA, FK506, caspofungin and their combinations. Data are expressed in arbitrary fluorescence unit (AU).

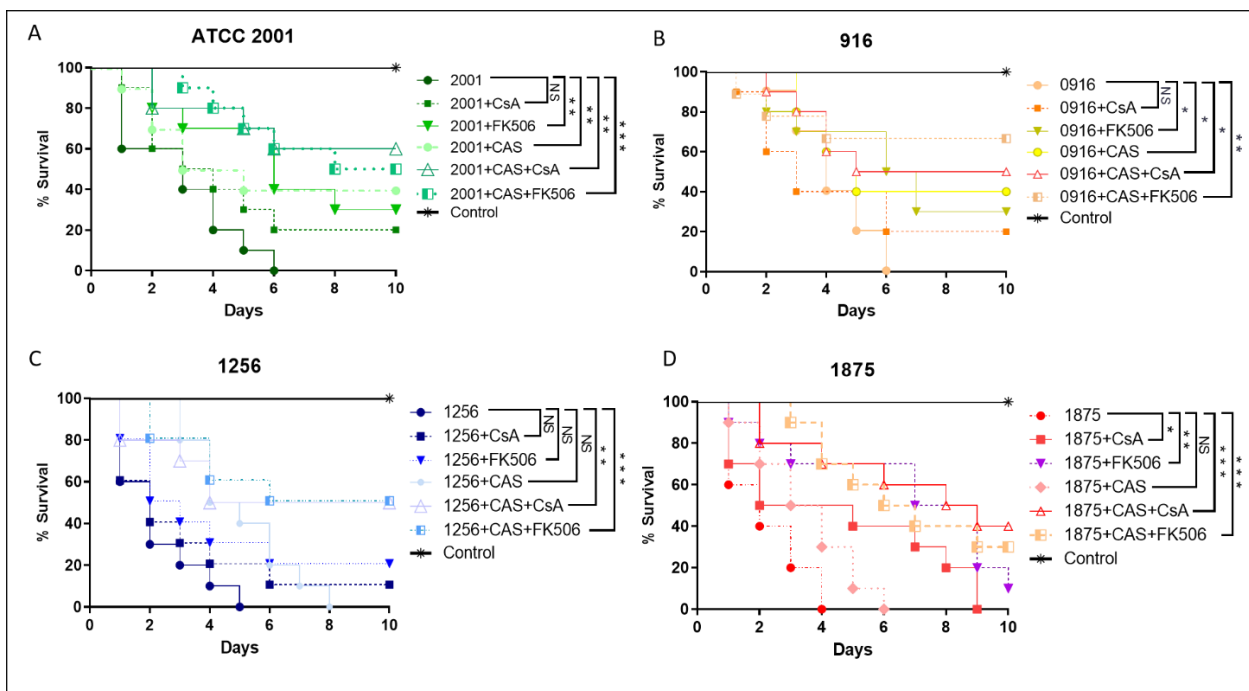


**Figure 7.** *Galleria* time-kill curves of caspofungin-susceptible (A, B) and resistant (C, D) *C. glabrata* isolates exposed to, caspofungin, calcineurin inhibitors and their combinations. The data are expressed as the percentages of survival. Log-rank (Mantel–Cox) test with p-values of < 0.05 was used to indicate statistical significance. As follows, \*p < 0.05, \*\*p < 0.02 and \*\*\*p < 0.001.